

Droplet evaporation during dropwise condensation due to deposited volatile organic compounds

Xiongjiang Yu,¹ Carlos Alberto Dorao,¹ and Maria Fernandino^{1, a)}

*Department of Energy and Process Engineering
Norwegian University of Science and Technology
N-7491, Trondheim, Norway.*

During dropwise condensation on a hydrophobic surface, it is intuitively assumed that droplets will grow with time. However, it can be observed that some droplets follow an opposite fate and instead disappear. This happens for example close to hygroscopic particles as they alter the local relative humidity. Here we show that evaporation of droplets during dropwise condensation on a smooth surface can occur due to local changes in the surface wettability. This local changes in the wettability are found to be a consequence of deposited volatile organic compounds (VOC) which create nanostructures in the region where a droplet was previously condensed and evaporated. A new droplet that forms or lands on the mentioned nanostructures experiences a suspended wetting state with a higher thermal resistance. This droplet can grow up to a critical size controlled by the contact resistance of the nano-structures and will then evaporate when surrounded by neighbouring colder droplets in a normal or partial wetting state.

Keywords: DWC, Evaporation, VOC, Nano structures, thermal resistance

When a cold surface is surrounded by a hot humid environment, droplet nucleation occurs and the droplets grow. However, in the presence of hygroscopic particles such as salt nucleus^{1,2}, propylene glycol³, nectars⁴ or ice drops⁵, the saturated vapor concentration between the hygroscopic particle and the condensation droplets can be altered. This situation leads to a dry zone near the hygroscopic particle and droplet nucleation is therefore hindered. Nath et al.⁵ attributed the dry zone to an inhibited nucleation and inhibited growth mechanisms. They observed that when new tiny droplets landed in the growth-inhibited region of an ice drop, they would finally evaporate.

Here, we show that during dropwise condensation on a smooth surface some droplets can evaporate even in the absence of any hygroscopic or ice particle. This phenomenon is attributed to local changes in the surface wettability. These local changes in the wettability are found to be a consequence of volatile organic compounds (VOCs) that create nano-structures in the region where previously a droplet was condensed and later evaporated. A new droplet that forms or lands on the mentioned nano-structures experiences a partial wetting state with a higher thermal resistance. Due to local differences in dew point and saturation conditions, droplets in a normal wetting state surrounding the droplet on a suspended wetting state consume the latter until it vanishes. The presence of VOCs after condensation-evaporation cycles also affect the droplet size distribution during subsequent condensation cycles.

Atmospheric volatile organic compounds (VOCs) are organic chemicals present in ambient air originating from volatilisation of solids and liquids from both natural and anthropogenic sources such as industrial pro-

cesses and energy production from hydrocarbons and bio-fuel combustion⁶⁻⁸. These VOCs can be deposited on solid surfaces by adsorption^{7,9} or condensation-assisted deposition¹⁰. Although the influence of VOCs on the change of intrinsic hydrophobicity by adsorption on a surface has been recognized in the literature^{11,12}, complete characterization of the process during vapor condensation has not been reported. Only recently have some studies reported the use of VOCs as a passive way of surface coating for promoting heterogeneous nucleation¹⁰ and to obtain stable superhydrophobic surfaces by depositing VOCs in consecutive condensation-evaporation cycles⁹. The fact that these VOCs can also be the cause of droplet evaporation during dropwise condensation has not been previously reported to our knowledge.

The study was performed with hydrophobic substrates that were prepared on a plain silicon wafer by vapor deposition of 1H,1H,2H,2H-perfluorooctylsilane. The substrate was placed on a programmable temperature-controlled cooling stage setting the surface temperature at $5 \pm 0.1^\circ\text{C}$ while the ambient temperature was measured to be 23.5°C with a relative humidity of 45% (dew point 10.9°C). These conditions corresponded to a sub-cooling of 5.9°C . Images of the condensation process were captured from the top using a Keyence VHF-950F digital microscope with a 500x long-working distance lens.

Evaporation of droplets on a condensation surface. The resulting condensation process at two different moments is depicted in Figure 1(a). From these two snapshots it is possible to observe that some droplets (droplets 4, 5 and 6 in the figure) grow while some other droplets (droplets 1, 2 and 3 in the figure) shrink during the period from $t=1350\text{s}$ to $t=1785\text{s}$. The time evolution of the diameters of the above selected droplets are shown in Figure 1(b), where droplets 4, 5 and 6 grow monotonously due to mass transfer or sharply by coalescence with neighboring droplets. Droplets 1, 2 and 3 show a similar growth rate until they reach a critical size,

^{a)} Electronic mail: maria.fernandino@ntnu.no

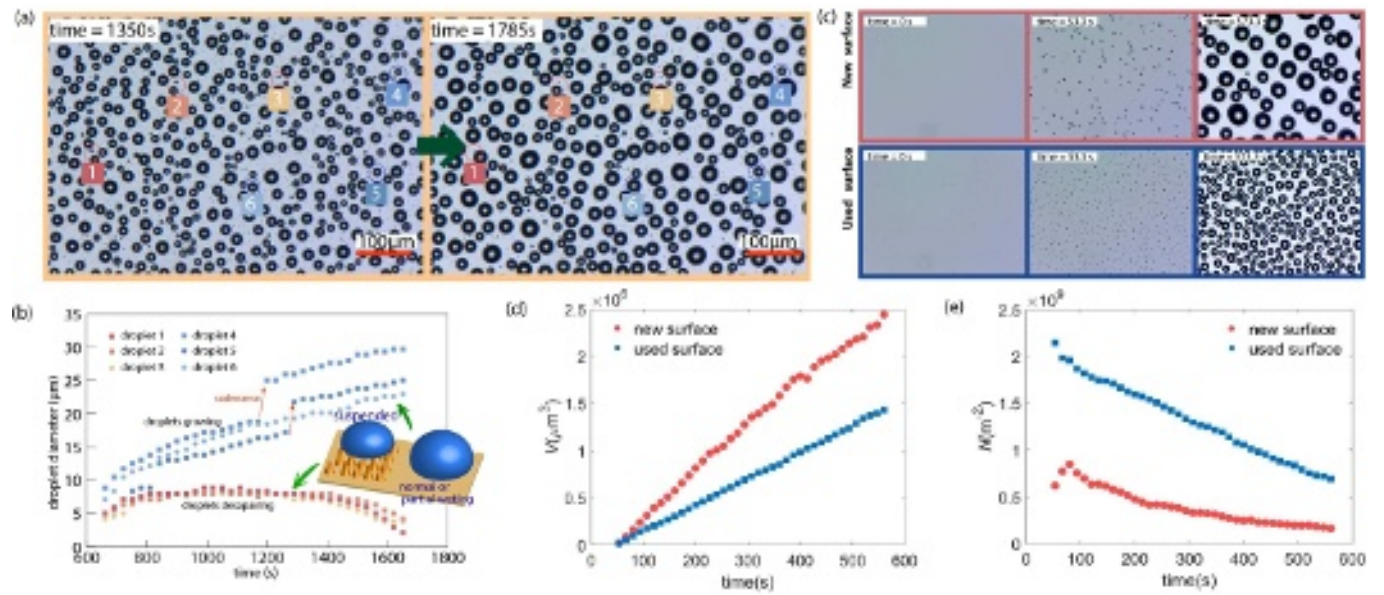


FIG. 1. Droplets evaporating on a nano-structured surface during condensation conditions: (a) visualization of the hydrophobic surface at different times; (b) temporal evolution of droplet diameters for two kinds of wetting states droplets; (c) comparison of droplet size and distribution on a new and an used surface; (d) comparison of averaged droplet size change rate on a new and a used surface; (e) comparison of droplet number density evolution on a new and on a used surface.

after which they cannot grow further. When the larger neighbouring droplets grow and get close to the droplet with impeded growth, the latter finally shrinks and evaporates completely. The initial limitation in the growth rate of some of the droplets can be attributed to local changes in the surface due to impurities, as schematically shown in Figure 1(b), adding an extra thermal resistance between the droplet and the surface and limiting their further growth by condensation.

In order to understand whether the behaviour of the droplets can be attributed to local changes in the surface, the condensation process on two surfaces were compared, see Figure 1(c)-(e). The first surface corresponds to a new plain hydrophobic surface while the second surface is a plain hydrophobic surface that has been exposed to 10 condensation-evaporation (condensation-drying) cycles. After these condensation-evaporation cycles, a certain amount of volatile organic compounds (VOCs) remain deposited on the surface (which will be characterized further down, see for instance Figure 3). Figure 1(c) shows the initially nucleated droplets at $t=53.5$ s for both surfaces. It is clearly observed that there is a much larger number of nucleated droplets on the used surface as compared to the new one, suggesting that changes in the surface after some condensation-evaporation cycles (i.e. deposited VOCs) is the cause of this increase in nucleation sites number. Basically, the deposited VOCs form micro/nano-structures on the sample surface, introducing a great number of nucleation cavities and decreasing the energy barrier needed for embryo formation. The higher initial nucleation number density in the used surface can be seen in Figure 1(e), where the initial peak

in the number of droplets for the used surface is up to 4 times larger than for the new surface. On the new surface, after the initial droplet nucleation due to condensation, no further new droplets are observed so that droplet growth and coalescence dominate the condensation process, with a consequent decrease in droplet density as observed in Figure 1(e). The rate of change in droplet number density decreases with time, since the distance between neighbouring droplets becomes larger as coalescence occurs. At $t=573.3$ s a low density of large droplets is observed. In the case of the used surface, after the initial condensation stage, some of the nucleated droplets stop growing and some evaporate, while other droplets keep growing and coalescing. The overall droplet density is much larger than for the plain surface, due to the existence of several small droplets as compared to the new surface. However, Figure 1(d) shows that the average droplet volume is larger for the new surface compared to the used one, suggesting an improved heat transfer for the former case. The deposited VOCs in the used surface generate nano/micro-structures that increase the thermal resistance between the condensing droplets and the base of the substrate, decreasing the growth rate of the droplets as compared to the new surface, as evidenced in Figure 1(d). With slower growth rate on the used surface, droplets here do not coalesce so often as on the new surface. On the other hand, coalescence is still possible with a smaller increase in droplet volume, since droplets lay much closer to each other in the used surface. The decrease in droplet number density for both surfaces in Figure 1(e) is mainly due to coalescence of droplets and evaporation of some droplets for the case of the used

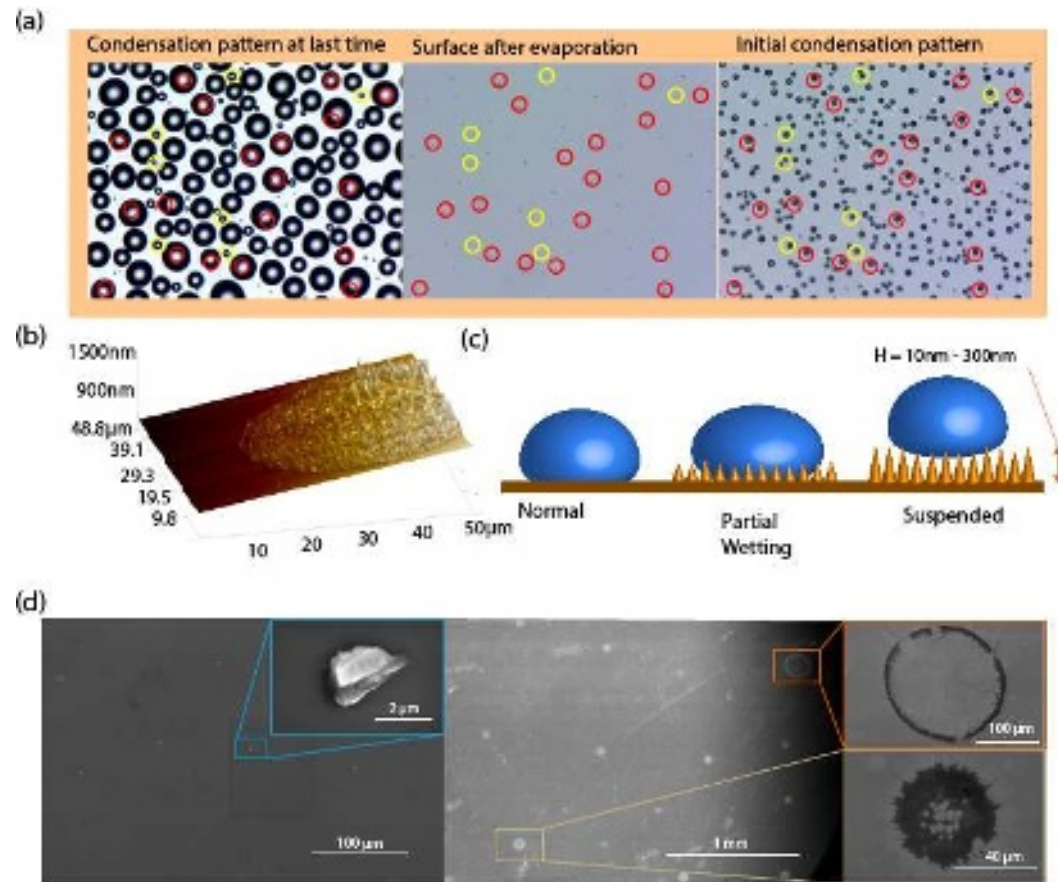


FIG. 2. (a) Condensation of droplets at 5.9°C subcooling, after 10 condensation/drying cycles on hydrophobic surfaces visualized under an optical microscope; (b) AFM image of VOCs deposited on the surface; (c) schematic diagram indicating three potential wetting states on the multi-wettability surface due to different morphological properties of the deposited VOCs; (d) three types of condensation-evaporation generated morphologies: (left) single-crystal type after 1 condensation/evaporation cycle, (center and right) ring-shaped hollow type (in red box) and ring-shape solid type (in yellow box) after 50 condensation/evaporation cycles.

surface, as it could be observed from the visualization video. In summary, these results indicate that the deposited VOCs affect the dropwise condensation process by initially providing more nucleation sites for droplets to form, but at the same time introducing an extra thermal resistance between the droplets and the substrate that hinders droplet growth and causes droplet evaporation.

Formation and visualisation of nano-structures.

In order to understand the cause of the fate of the disappearing droplets, the changes in the surface during condensation were studied. It is known that volatile organic compounds VOCs are found mixed with non-condensable gases^{13,14} and nanoscale agglomerates can be deposited on the surface. For example, Cha et. al¹⁰ make use of such VOCs to fabricate nanoscale agglomerates on a hydrophobic surface for the promotion of condensation nucleation.

To study the possible formation of VOCs nano-structures in our study, a new surface is exposed to condensation-evaporation cycles. After 10 condensation/drying cycles on a surface exposed to humid air, dot

patterns detectable by optical microscopy are observed on the surface. Similar patterns have been previously observed in the literature¹⁰. However, most of the nano-features that can be related to the further condensation of droplets¹⁵, can be too small to be observed by the optical microscope. Figure 2(a) shows the nucleation and condensation pattern during a condensation/drying cycle. Red circles in the figure show nucleation of droplets on visible dots on a dry surface before the condensation takes place. Yellow circles in the figure show the nucleation of droplets on non-noticeable visible dots under the microscope. However, the nucleation at the same location when the condensation cycle is repeated (last picture in Fig. 2(a)), indicates the presence of nanostructures acting as nucleation points even when not visible under the microscope.

By investigating the surface after several condensation/evaporation cycles with atomic force microscopy (AFM) as shown in Fig. 2(b), it is possible to observe the formation of nano-structured regions. In these regions, the density and height of the nano-structures are

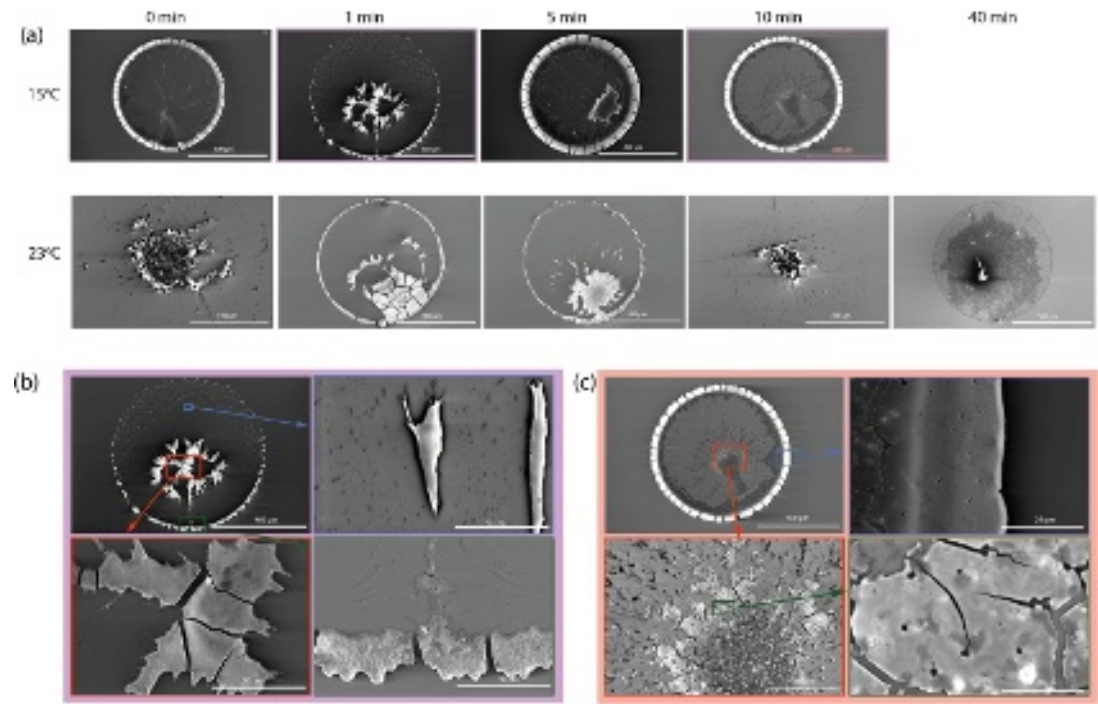


FIG. 3. Evolution of VOCs structures with time: (a) the overview of VOCs structures left after the drop evaporation with increasing absorbing time under two different surface temperatures; (b) and (c) zoom-in images showing porous nature of VOCs structures

not uniform. In the central part of the nano-rough region, the nano-structures are sparsely distributed and the height is about 10 nm, while in some edge parts of the nano-rough region, the nano-structures are densely distributed and the heights of the structures reach up to about 300 nm. Fig. 2(d) shows the morphology of the deposited structure developed after the condensation/evaporation cycles. After a first time cycle, a microstructure is sparsely distributed in the form of single crystals of about $1 \mu\text{m}$ in size. With more cycles taking place, more VOCs keep depositing onto the surface. After approximately 50 cycles, two types of ring-shape patterns were observed, namely a hollow and a solid type. The area covered by the deposited structures is of the order of hundreds of micrometers. The formation process of solid VOCs nano-structures is complex. Many factors can affect the final pattern, such as the total amount of VOCs within a single drop¹⁶ and the flow pattern inside the droplet during crystallization^{16,17}. The total amount of VOCs within a single drop is related to the absorbing time as well as the droplet temperature which determines the solubility. The flow pattern inside the droplet during evaporation is related to the droplet size, shape, temperature and contact angle. We performed further experiments to show how the formed microstructures change with increasing absorbing time under two different temperatures. Every time, a $1 \mu\text{L}$ droplet was put onto the hydrophobic surface by a micro syringe in an environment of $23 \text{ }^\circ\text{C}$ with relative humidity of 32 %. Two initial surface temperatures were tested, namely 23

$^\circ\text{C}$ and $15 \text{ }^\circ\text{C}$. The deposited droplet was left at rest for a period of 0 to 40 minutes in order to vary the absorbing time. After this time, the surface temperature was increased to $60 \text{ }^\circ\text{C}$ with a slope of $20 \text{ }^\circ\text{C}$ per minute to let the droplet evaporate. The SEM images of the generated microstructures for different droplet deposition times are shown in Fig. 3(a). Since the lifetime of a 1 microliter droplet on the hydrophobic surface in an environment of $\text{RH}=35\%$ and $T=23 \text{ }^\circ\text{C}$ is about 14 minutes, no picture is available for 40 minutes absorption time for this case.

As it can be seen from Figure 3(a), VOCs can be deposited in a ring-shape manner around the droplet contact line, concentrated in the droplet center or more uniformly distributed throughout the droplet base. A more evident ring-shaped deposition pattern is observed for the higher temperature, while a more mountain-like deposition takes place at lower temperatures, in accordance with the observations reported by Gregson et al.¹⁸. At the same time, increasing the absorption time may lead to the increase of VOCs concentration inside the droplet if the drop is initially unsaturated. Higher concentration has been reported to result in more deposition on the area inside the outer ring¹⁸, which can explain the larger deposits of VOCs observed for longer times in Fig 3(a). However, the final deposition pattern is a complex interaction between evaporation-induced internal flow, contact line pinning, total amount of VOCs (which depends on the absorbing time and temperatures) and the accumulation speed of VOCs (which also depends on the evaporating temperatures). The investigation of the fi-

nal deposition pattern lies outside the scope of this study and the reader is referred to the more specialised literature on the topic for further details^{18–20}. Despite the different distribution of the deposited microstructures, they are all porous structures in the size of a few micrometers or sub micrometers as shown in the zoom-in images of Fig. 3 (b) and (c). These porous structures have a larger thermal resistance than the metallic smooth substrate. Therefore, once a droplet of a few micrometers in diameter is located on the porous structures, the droplet is expected to be evaporated due to the local higher temperature as well as corresponding higher saturated vapor pressure compared to the ones located on the bare part of the surface.

Droplet dynamics on VOCs nanostructures. To better clarify the role that VOCs play on the droplet dynamics during condensation, we performed further condensation experiments comparing a new, clean surface with a surface fully covered with VOCs. This enabled us to distinguish between droplets lying on the smooth surface or on the VOCs part. We cut a new hydrophobic silicon wafer into 2 parts. One part, referred to as the clean, new surface, was placed on the cooling stage. With an ambient temperature of $T=22^{\circ}\text{C}$ and relative humidity of $RH=35\%$, corresponding to a dew point of 6°C , the substrate temperature was set to 5°C . The condensation process was recorded for 10 minutes. The images before and after 10 minutes condensation are shown in Fig. 4(a) and (b), respectively. For the second part of the hydrophobic silicon wafer, a big DI water droplet of around 6 mm in diameter was deposited onto the surface to absorb VOCs for 1 hour at ambient conditions ($T=22^{\circ}\text{C}$ and relative humidity of $RH=35\%$), as shown in Fig. 4(c). After this time, the substrate temperature was increased to 60°C with a slope of 20°C per minute to let the droplet evaporate. The residual VOCs pattern after complete droplet evaporation is shown in Fig. 4(d). It should be noted that the VOCs are very obvious in Fig. 4(e) even before the condensation take place, which differs from Fig. 2. This is an expected result since the amount of VOCs in a single droplet is proportional to its volume and increases sharply with droplet size under the same solubility. The same condensation process as described for the first clean substrate was then repeated with this VOCs surface. The recorded images before and after 10 minutes condensation are shown in Fig. 4(e) and (f), respectively. By comparing Fig. 4 (b) and (f), we confirm that the VOCs on a hydrophobic surface can increase droplet nucleation density but at the same time will also lead to smaller droplet sizes during dropwise condensation, consistent with our previous observations.

Figure 4(f) shows that droplets can nucleate on the VOCs structures, but most of them cannot grow further than several micrometers in diameter. This phenomenon is similar to what was observed in our condensation experiments shown in Fig. 1(a), where some of the depicted droplets stop growing and then evaporate as condensation continues in the rest of the surface. For a droplet

to continue growing, there must be a local positive subcooling below the dew point. Assuming a constant humidity and temperature everywhere before the condensation starts, a droplet will nucleate when the subcooling is enough to overcome the local energy barrier for nucleation. Once nucleated, the droplet will start growing due to further condensation of the surrounding vapour. However, the local vapor concentration around a droplet is decreased by its neighbouring droplets who also absorbed vapor molecules from the environment. In this way, the local vapor concentration and the local dew point around a droplet will keep decreasing, generating a gradient of vapour concentration decreasing towards the solid wall. If all the droplets had the same temperature, they would keep growing due to the same vapor diffusion gradient. However, droplets lying over VOCs regions will have a slightly higher temperature than the ones lying on the clean substrate due to the extra thermal resistance introduced by the VOCs. The colder droplets will cause the local vapour concentration to be equal or lower than the saturated vapor conditions for the warmer neighbouring droplets. Accordingly, the latter will stop growing and may even evaporate.

In terms of the extra thermal resistance introduced by the VOCs, Rykaczewski et.al²¹ proposed a volumetric roughness parameter R_v for characterizing this generated nano-roughness. This parameter is defined as the height of a liquid film with volume equal to the fill volume between the nano-structures. In their study, if R_v is larger than 35 nm the droplets can be in a suspended state. Below this number, the liquid body can reach the bottom of the surface adopting a partial wetting state. In our case, with a R_v factor ranging from 7.4 nm to 221.5 nm it is expected that some droplets will be in a suspended state while some others will be in a partial wetting state. Figure 2(c) shows a schematic representation of the possible wetting states of a droplet in the presence of these nano-structures. Since the nano-structures are sparsely distributed on the surface, droplets can also be found in direct contact with the smooth surface, what we here call a "normal" wetting state.

Another point to consider is that during the condensation process droplets can also grow within the nano-structures and finally flood the nano-structures²², especially under large subcooling conditions ($\Delta T \gtrsim 3.0\text{ K}$). However, droplets can remain in a suspended state at small subcooling temperatures²² ($\Delta T=0.3\text{ K}$). This can be explained by the minimum droplet size for nucleation to happen, expressed as²³ $r_{min} = 2T_{sat}\sigma/(h_{fg}\rho_l\Delta T)$, where T_{sat} , σ , h_{fg} , ρ_l and ΔT are the saturation vapor temperature, liquid-vapor surface tension, latent heat of vaporization, liquid density and subcooling temperature (i.e. the temperature difference between the saturation temperature and the liquid droplet temperature), respectively. Under large subcooling conditions, the minimum droplet size required for nucleation can be small enough to enable new droplets nucleated within the narrow space between nano-structures. As the droplet keeps growing,

This is the author's peer reviewed, accepted manuscript. However, the online version of record will be different from this version once it has been copyedited and typeset.
PLEASE CITE THIS ARTICLE AS DOI:10.1063/1.50056005

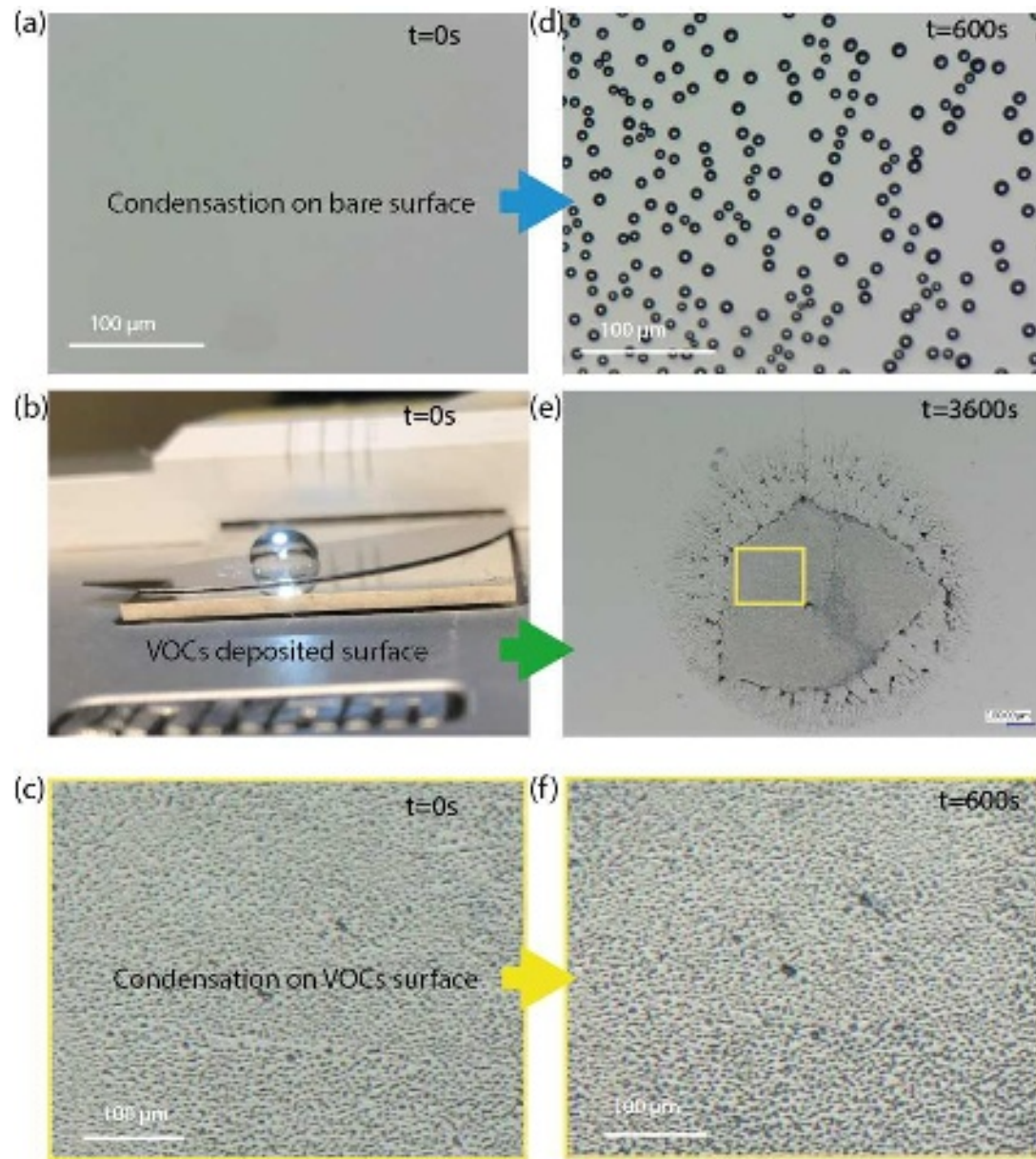


FIG. 4. (a) A new hydrophobic surface before condensation take place. (b) condensation droplets on the new hydrophobic surface after 600s. (c) A water droplet on the new hydrophobic surface absorbing VOCs in the environment. (d) VOCs left on the surface after the droplet evaporate completely. (e) zoom-in photo of (d), showing the surface where fully covered by VOCs (f) condensation droplets on the VOCs surface under same condensation parameters of (b), showing denser droplet population as well as smaller droplet sizes compared with that of new hydrophobic surface as shown in (b)

the nano-structure will eventually be flooded. On the other hand, under small subcooling conditions, the minimum droplet size needed for nucleation is larger than the space within the nano structures. Then the new droplets will form on top of the nano-structures. Based on the morphology of the nano-structures observed in this study (Fig. 2(b)), it is possible for droplets to nucleate either within the structures at the edges of the more sparsely distributed nano-structures and subsequently showing a partial wetting state (Fig. 2(c)) or above the structures in more dense nano-structured regions, where the space

inside the nano-structures is smaller than the minimum space required for a new droplet to form. In the latter case, if the roughness of the nano-structures is above the critical value of R_v previously described, the newly formed droplets are expected to grow in the suspended wetting state, as shown on the right of Fig. 2(c).

To understand the cause of the different behavior of the droplets showing a suspended or partial wetting state (Fig. 2(c)), the total thermal resistance in these two situations can be estimated. The total thermal resistance R_t from the water vapor to the condensation sur-

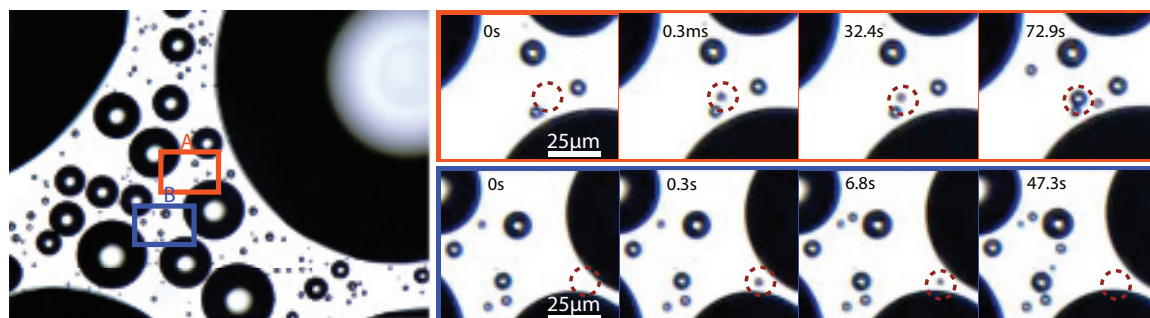


FIG. 5. Two contrary behaviours of newly landed droplets: growing droplet in the yellow box and evaporating droplet in the blue box in high humid environment of RH=75%, T=25°C.

face can be expressed as: $R_t = R_{int} + R_{cuv} + R_d + R_n$ with R_{int} , R_{cuv} , R_d , R_n the interfacial thermal resistance, curvature resistance, conductive resistance and nano-structure thermal resistance, respectively²⁴. Assuming a droplet of 5 μm radius in a suspended state in the humid air environment at 25 °C, the dominant thermal resistances are $R_d \approx 1.4 \times 10^{-6} \text{m}^2 \text{K/W}$ and $R_n \approx 4.3 \times 10^{-6} \text{m}^2 \text{K/W}$, where the last value is estimated assuming that all the conductive heat is through a gas layer of about 100 nm in the nano-structures. However, this thermal resistance can be expected to be higher as the mean free path of air molecules at 1 bar and at 20°C is about 65 nm²⁵ which is comparable to the trapped gas layer of ≈ 100 nm in the contact region. Consequently, due to the large value of the nano-structures thermal resistance R_n , the VOCs structures decrease the subcooling temperature between the water droplet and the humid environment by providing an extra temperature drop from the droplet to substrate. Droplets in a suspended state will therefore be warmer than droplets in a partial or normal wetting state. When the local humidity of the warmer droplet further decreases due to the approach of surrounding colder droplets, both the local dew point and subcooling temperature of the warmer droplets decrease. Sometimes the subcooling temperature even becomes negative which corresponds to the case of evaporating droplets. This fact suggests that colder droplets in a partial or normal wetting state can absorb surrounding warmer droplets in a suspended state.

Behaviour for newly landed droplets. Previous studies have suggested that the droplet condensation behavior can be affected by the accumulation of non-condensable gasses (NCGs) near the condensing surface. Since water vapor concentration in the region close to the surface will decrease due to condensation of water on the surface, this region will be enriched in NCGs, that will in turn affect the speed of condensation by adding an extra resistance close to the surface. If the layer of NCGs is thicker than the height of some droplets lying on the surface, these droplets will be surrounded by NCGs and their growth will be hindered, sometimes also evaporating. Following this idea, a large droplet would keep growing while small droplets next to it would tend to shrink.

To elucidate whether the role of the non-condensable gases is responsible for the phenomenon reported in this work, small droplets were forced to be deposited on the condensation surface by increasing the humidity of the condensation chamber following the approach suggested in a previous study⁵. After 2 hours in a high humidity environment, as shown in the left part of Fig. 5, the condensation surface was covered by random sized droplets. Special attention is put on the dynamics of newly landed droplets on the condensation surface with the humid air. No new droplet was observed at $t=0$ s within the red marked area in the picture. New droplets landed at $t=0.3$ s and kept growing until $t=72.9$ s. It can also be noticed that there is an evaporating droplet located at the south west edge of the red circle in the picture of $t=0$ s. The initial size of this droplet is larger than the newly landed one. However, it turns out that the newly landed small droplet grows while the big one evaporates. If the non-condensable gases would dominate the droplet mass transfer process, this is an unexpected trend. On the other hand, this effect can be explained assuming that the droplet has landed on a region with nano-structures and that the droplet is in a suspended wetting state. Another example of a newly landed droplet evaporating is shown in the blue box of Fig. 5. Initially, there are no droplets at $t=0$ s in this region. A new droplet landed at $t=0.3$ s. However, instead of growing further, the new droplet evaporates after landing on the condensation surface. In this case, the effect of both NCGs and a suspended wetting state of the droplet on a nano-structured region need to be taken into account to describe the droplet behavior.

In this work, we show that during dropwise condensation on a smooth surface some droplets can evaporate. This phenomenon, which cannot be explained only by the accumulation of NCGs close to the surface, is attributed to the local changes in the surface wettability due to deposition of volatile organic compounds (VOCs) that create nano-structures in the region where a droplet has previously been condensed and evaporated. Volatile organic compounds promote the evaporation of droplets during dropwise condensation by generating local changes in the surface structure which results in suspended wetting state droplets. Due to the extra thermal resistance, these

droplets are warmer than surrounding droplets. These induced changes in local temperature and corresponding dew point when colder neighbouring droplets are growing by condensation, results in the evaporation of the suspended droplets. At the same time, the VOCs provide extra nucleation sites and result in a higher droplet density than would be present in a new, smooth surface. However, due to the extra thermal resistance introduced by the VOCs, droplet growth rate is slower, so that a surface that has already undergone some condensation cycles, ends up with a larger number of droplets smaller in size than for a new surface. The results from this work demonstrate that deposition of VOCs can alter the local wetting conditions and overall condensation pattern, which is relevant in practical condensation applications.

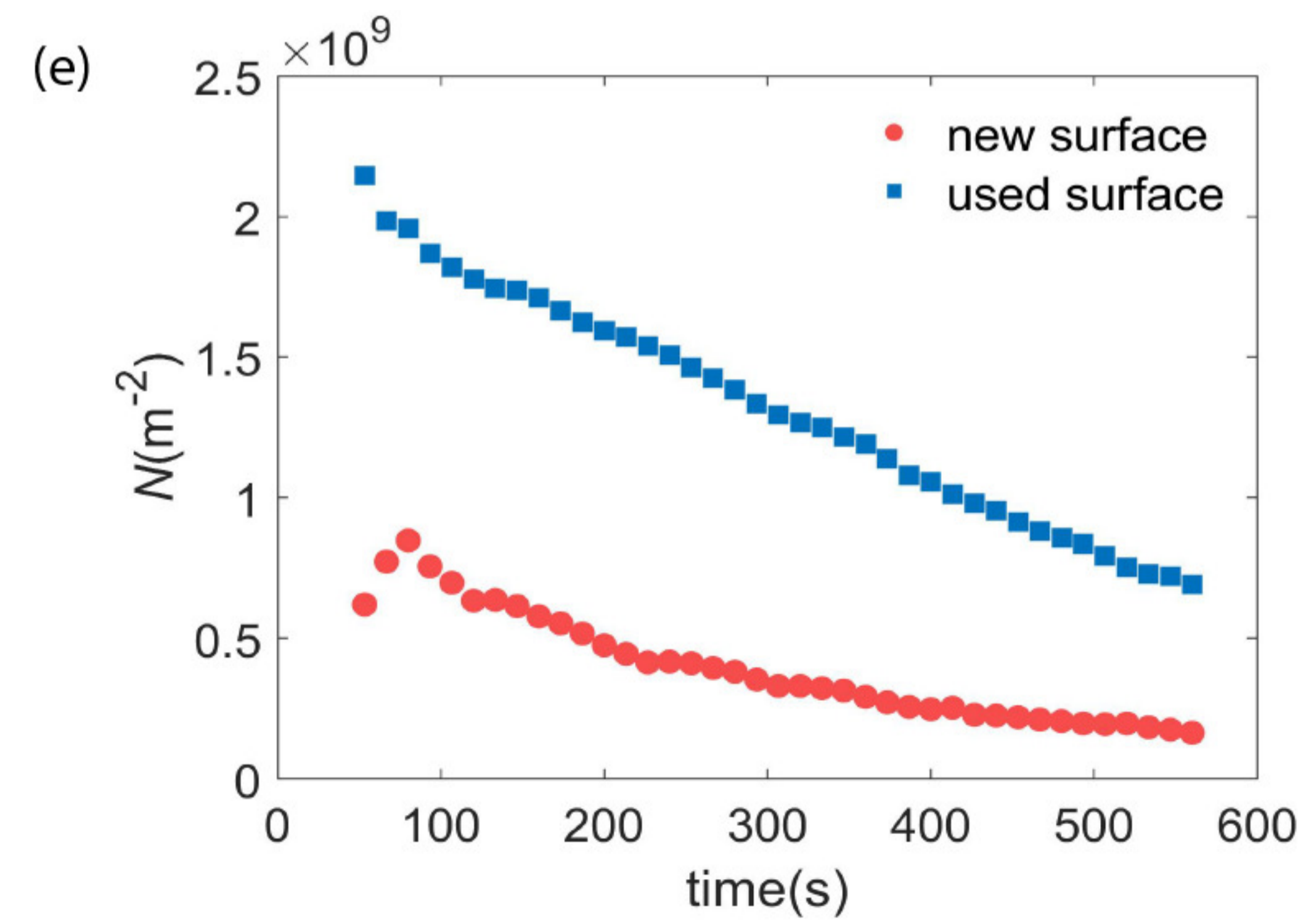
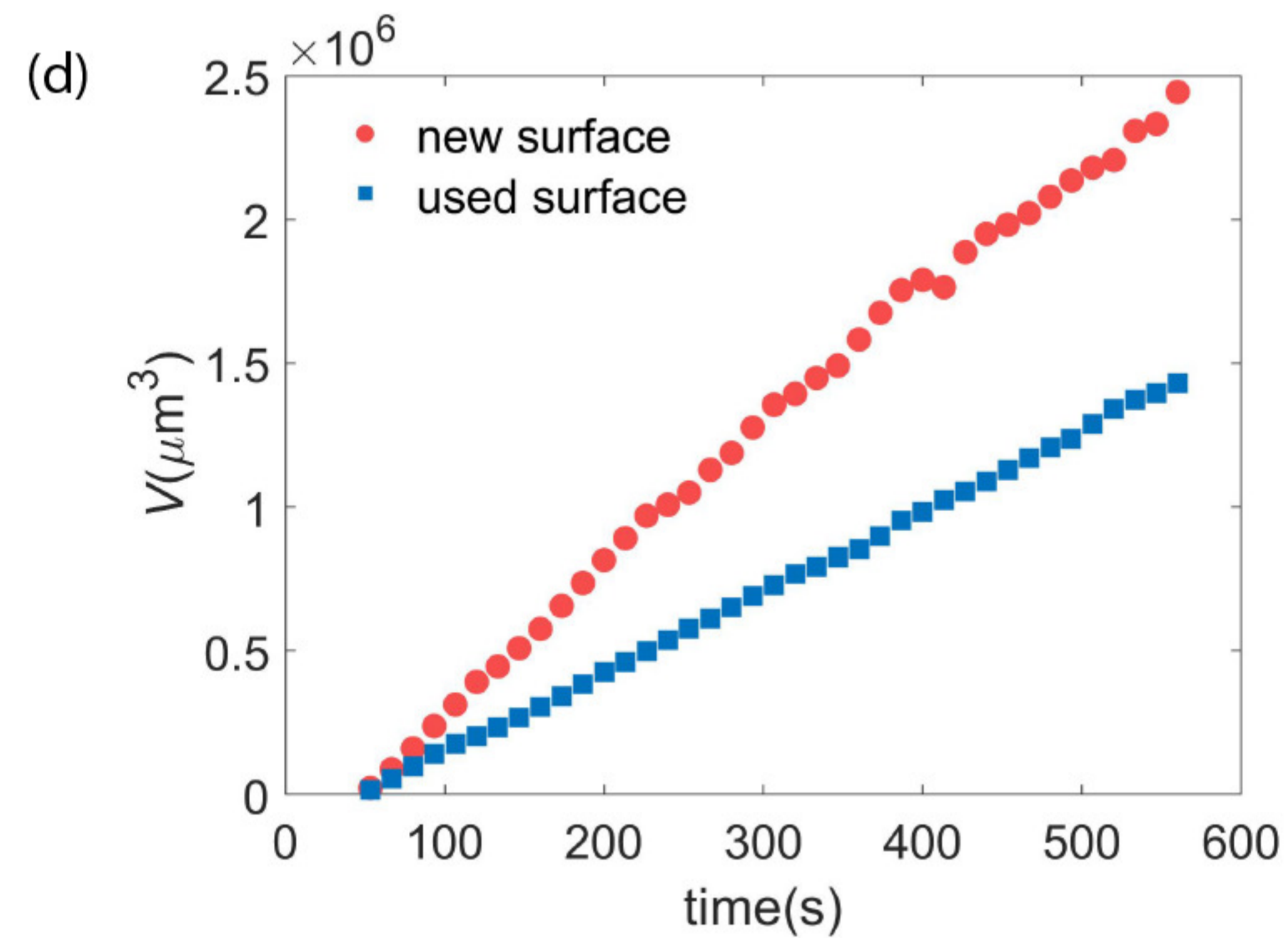
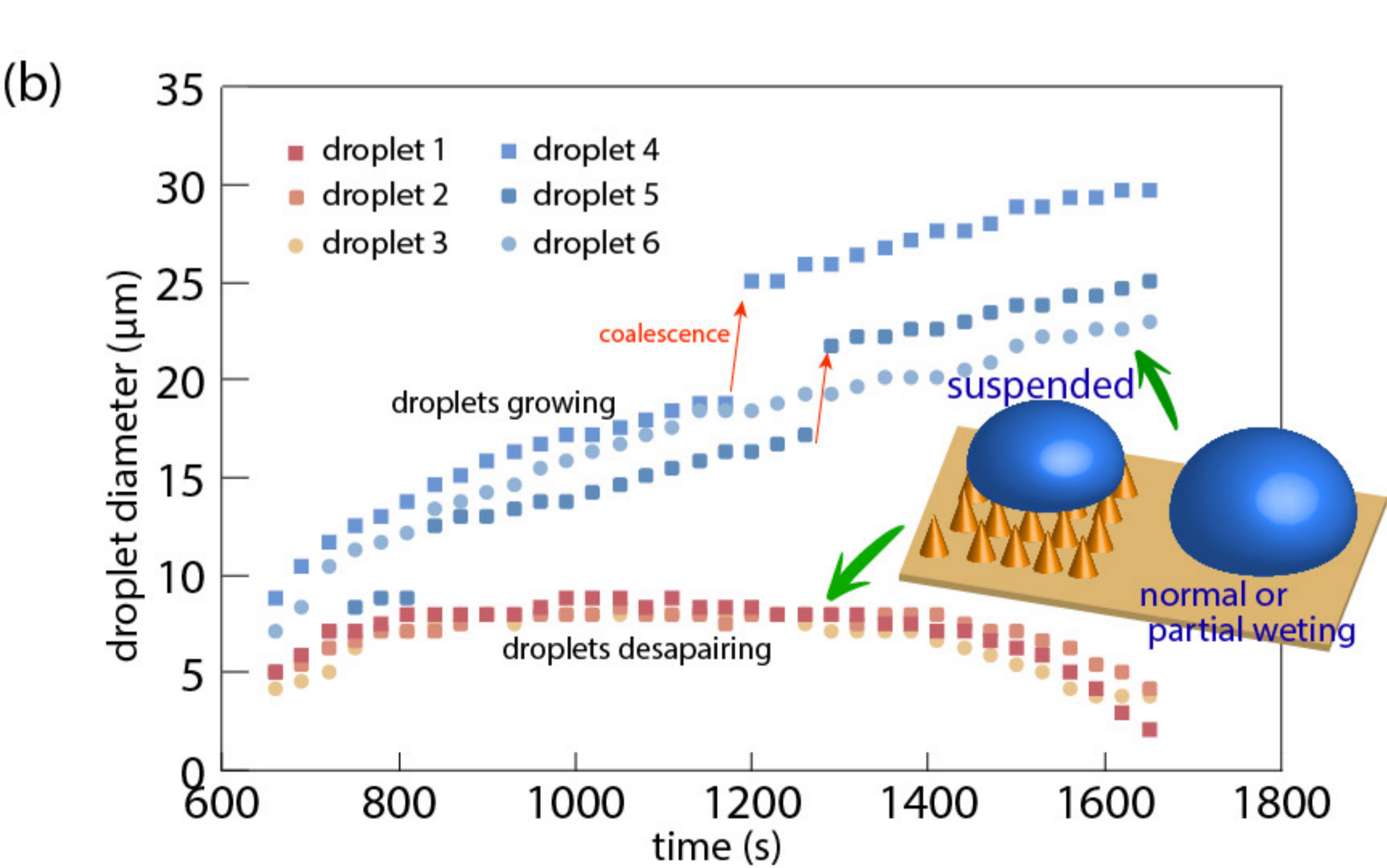
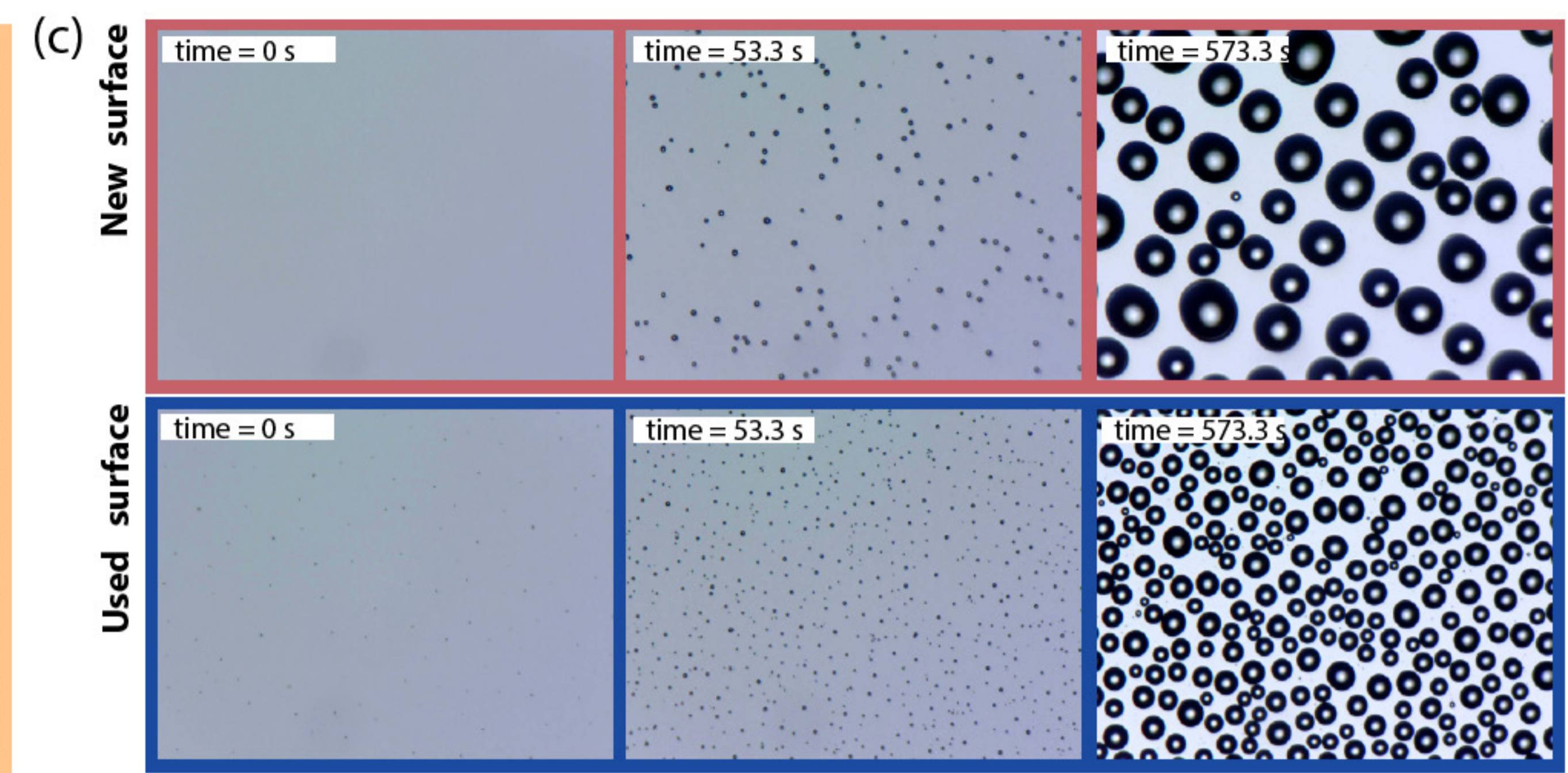
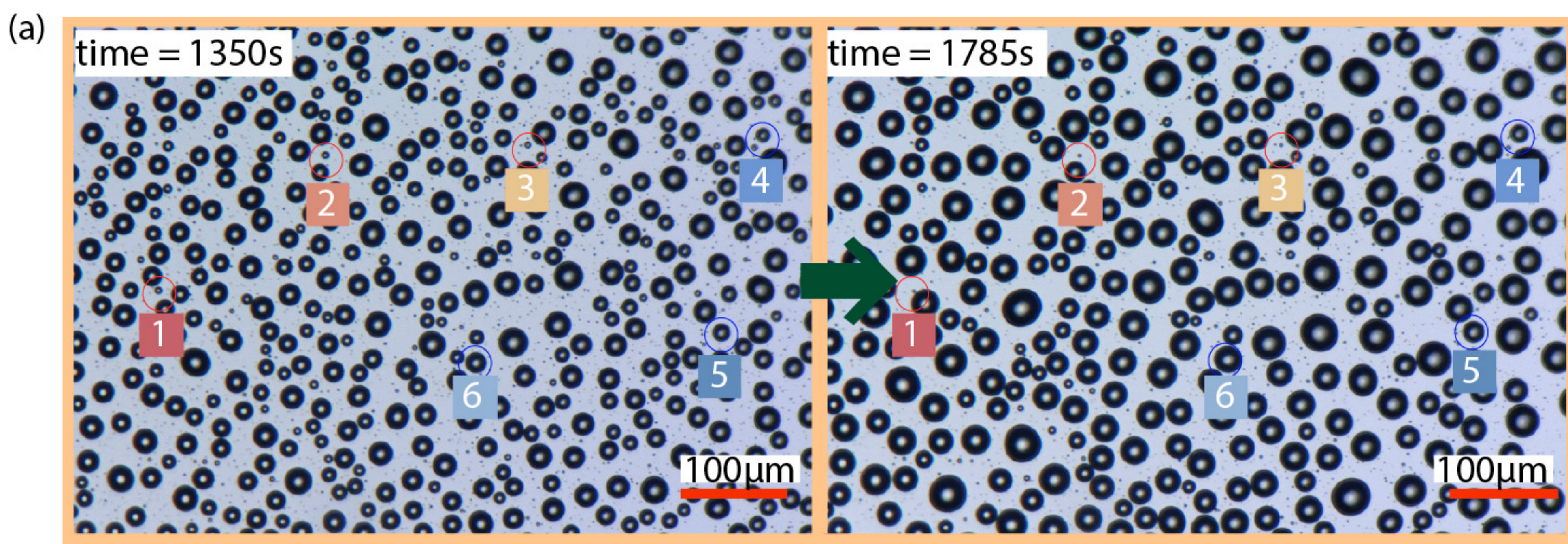
Supplementary Material See supplementary material for the details of the experimental facility and preparation of the samples.

Acknowledgement The Research Council of Norway is acknowledged for the project number 275587 and for the support to the Norwegian Micro- and Nano-Fabrication Facility, NorFab, project number 295864.

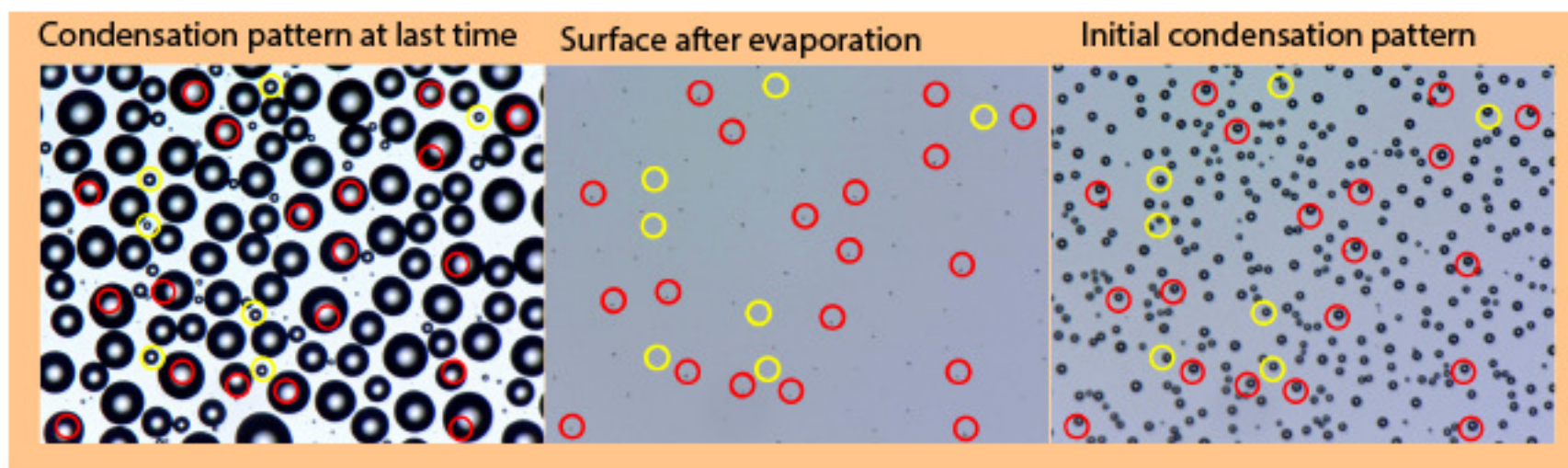
Data availability The data are available from the corresponding author upon reasonable request.

References

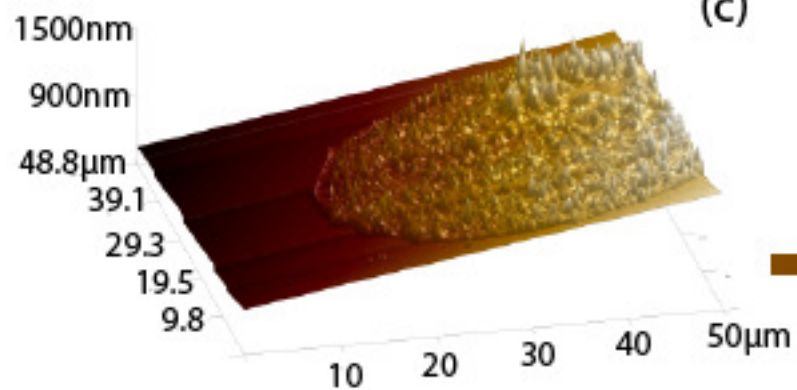
- ¹R. Williams and J. Blanc, "Inhibition of water condensation by a soluble salt nucleus," *J. Chem. Phys.* **74**, 4675–4677 (1981).
- ²J. Guadarrama-Cetina, R. D. Narhe, D. A. Beysens, and W. Gonzalez-Viñas, "Droplet pattern and condensation gradient around a humidity sink," *Phys. Rev. E* **89**, 012402 (2014).
- ³X. Sun, A. Damel, V.G. and Uppal, R. Linder, S. Chandrasekar, A. Mohan, and K. Rykaczewski, "Inhibition of condensation frosting by arrays of hygroscopic antifreeze drops," *Langmuir* **31**, 13743–13752 (2015).
- ⁴S. Biswas, A. Chakrabarti, and A. Chateauminois, "Soft lithography using nectar droplets," *Langmuir* **31**, 13155–13164 (2015).
- ⁵S. Nath, C. Bisbano, P. Yue, and J. Boreyko, "Duelling dry zones around hygroscopic droplets," *J. Fluid Mech.* **853**, 601–620 (2018).
- ⁶S.-M. Li, A. Leithead, S. Moussa, J. Liggio, M. Moran, D. Wang, K. Hayden, A. Darlington, M. Gordon, R. Staebler, P. Makar, C. Stroud, R. McLaren, P. Liu, J. O'Brien, R. Mittermeier, J. Zhang, G. Marson, S. Cober, M. Wolde, and J. Wentzell, "Differences between measured and reported volatile organic compound emissions from oil sands facilities in Alberta, Canada," *Proceedings of the National Academy of Sciences* (2017).
- ⁷X. Zhang, B. Gao, A. Creamer, C. Cao, and Y. Li, "Adsorption of VOCs onto engineering carbon materials: a review," *Journal of Hazardous Materials* **338**, 102–123 (2017).
- ⁸T. Adamova, J. Hradecky, and M. Panek, "Volatile organic compounds (VOCs) from wood and wood-based panels: Methods for evaluation, potential health risks, and mitigation," *Polymers* **12**, 2289 (2020).
- ⁹X. Yan, Z. Huang, S. Sett, J. Oh, H. Cha, I. Li, L. Feng, Y. Wu, C. Zhao, D. Orejon, F. Chen, and N. Miljkovic, "Atmosphere-mediated superhydrophobicity of rationally designed micro/nanostructured surfaces," *ACS Nano* **13**, 4160–4173 (2019).
- ¹⁰H. Cha, A. Wu, M. Kim, K. Saigusa, A. Liu, and N. Miljkovic, "Nanoscale-agglomerate-mediated heterogeneous nucleation," *Nano Lett* **17**, 7544–7551 (2017).
- ¹¹D. Preston, N. Miljkovic, J. Sack, R. Enright, J. Queeney, and E. Wang, "Effect of hydrocarbon adsorption on the wettability of rare earth oxide ceramics," *Applied Physics Letters* **105**, 011601 (2014).
- ¹²J. Ma, S. Sett, H. Cha, X. Yan, L. Feng, Y. Wu, C. Zhao, D. Orejon, F. Chen, and N. Miljkovic, "Atmosphere-mediated superhydrophobicity of rationally designed micro/nanostructured surfaces," *ACS Nano* **13**, 4160–4173 (2019).
- ¹³C. McDonald, J. B. Gouw, J.A. and Gilman, S. H. Jathar, A. Akherati, C. Cappa, J. Jimenez, J. Lee-Taylor, P. L. Hayes, S. McKeen, Y. Cui, S. Kim, D. Isaacman-VanWertz, A. Goldstein, R. A. Harley, G. J. Frost, J. M. Roberts, T. B. Ryerson, and M. Trainer, "Volatile chemical products emerging as largest petrochemical source of urban organic emissions," *Science* **359**, 760 (2018).
- ¹⁴S. Gligorovski and J. Abbatt, "An indoor chemical cocktail," *Science* **359**, 632 (2018).
- ¹⁵G. Lopez, H. Biebuyck, C. Frisbie, and G. Whitesides, "Imaging of features on surfaces by condensation figures," *Science* **260**, 647–649 (1993).
- ¹⁶T. Bigioni, X. Lin, T. Nguyen, E. Corwin, T. Witten, and H. Jaeger, "Kinetically driven self assembly of highly ordered nanoparticle monolayers," *Nature Materials* **5**, 265–270 (2006).
- ¹⁷R. Deegan, O. Bakajin, T. Dupont, G. Huber, S. Nagel, and T. Witten, "Capillary flow as the cause of ring stains from dried liquid drops," *Nature* **389**, 827–829 (1997).
- ¹⁸F. K. A. Gregson, J. F. Robinson, R. E. H. Miles, C. P. Royall, and J. P. Reid, "Drying and crystallization of evaporating sodium nitrate aerosol droplets," *J. Phys. Chem. B* **124**, 6024–6036 (2020).
- ¹⁹X. Yang, Z. Jiang, P. Lyu, Z. Ding, and X. Man, "Deposition pattern of drying droplets," *Commun. Theor. Phys.* **73**, 047601 (2021).
- ²⁰R. Malonowski, G. Volpe, I. P. Parkin, and G. Volpe, "Dynamic control of particle deposition in evaporating droplets by an external point source of vapor," *J. Phys. Chem. Lett.* **9**, 659–664 (2018).
- ²¹K. Rykaczewski, W. Osborn, J. Chinn, M. Walker, J. Scott, W. Jones, C. Hao, S. Yao, and Z. Wang, "How nanorough is rough enough to make a surface superhydrophobic during water condensation?" *Soft Matter* **8**, 8786 (2012).
- ²²R. Wen, Z. Lan, B. Peng, W. Xu, R. Yang, and X. Ma, "Wetting transition of condensed droplets on nanostructured superhydrophobic surfaces: Coordination of surface properties and condensing conditions," *ACS Appl. Mater. Interfaces* **9**, 13770–13777 (2017).
- ²³J. R. Maa, "Drop size distribution and heat-flux of dropwise condensation," *Chem. Eng. J.* **16**, 171–176 (1978).
- ²⁴N. Miljkovic, R. Enright, and E. Wang, "Effect of droplet morphology on growth dynamics and heat transfer during condensation on superhydrophobic nanostructured surfaces," *ACS Nano* **6**, 1776–1785 (2012).
- ²⁵S. Jennings, "The mean free path in air," *Journal of Aerosol Science* **19**, 159 (1988).



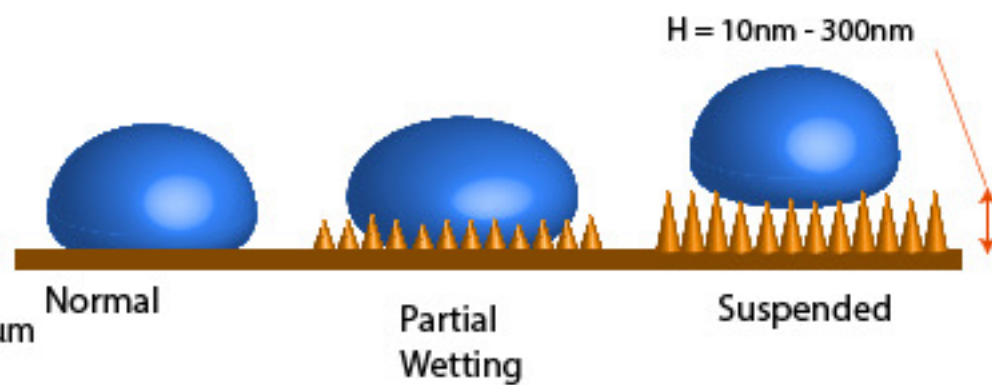
(a)



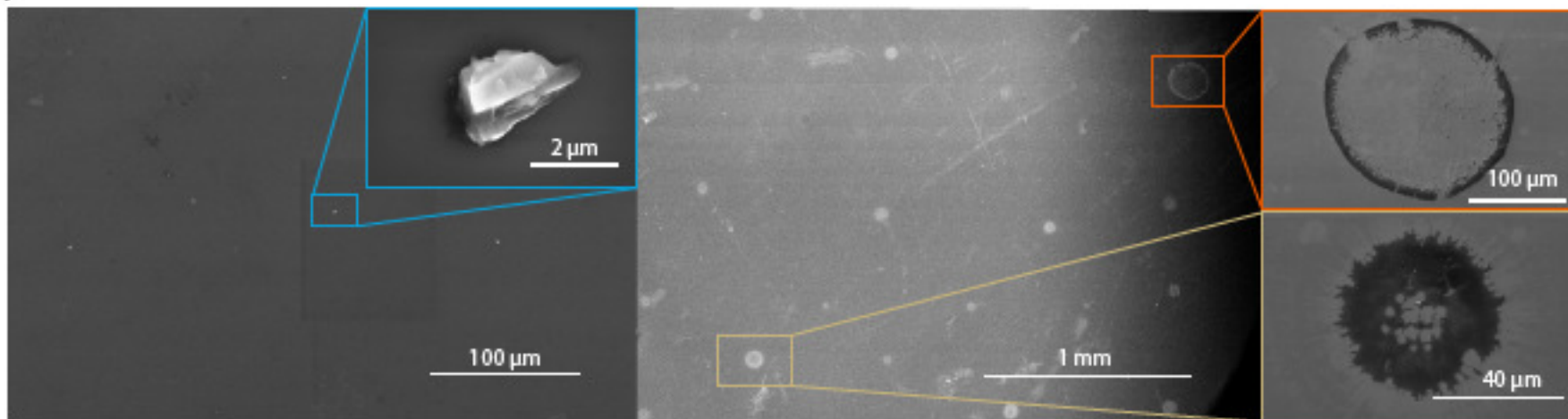
(b)

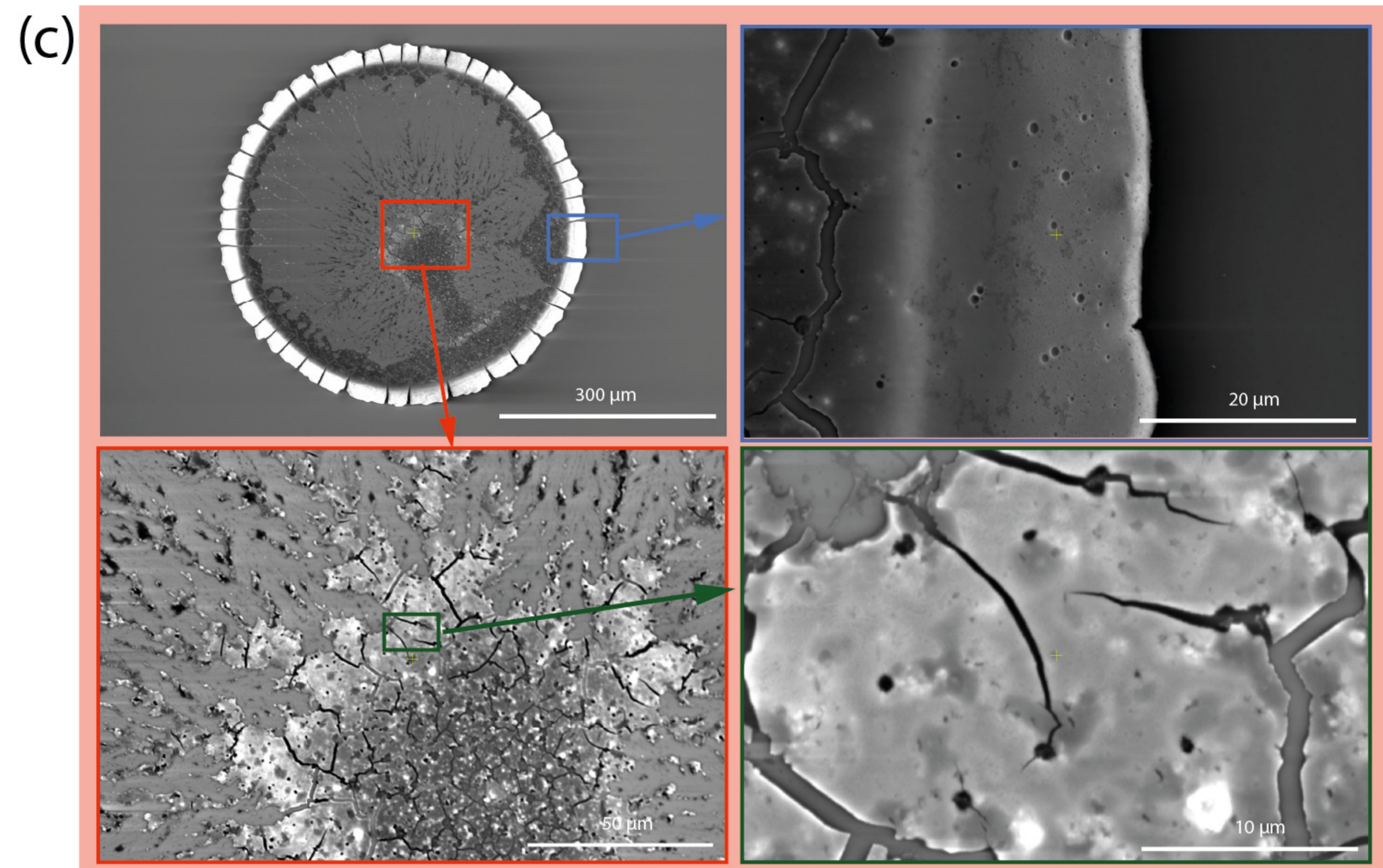
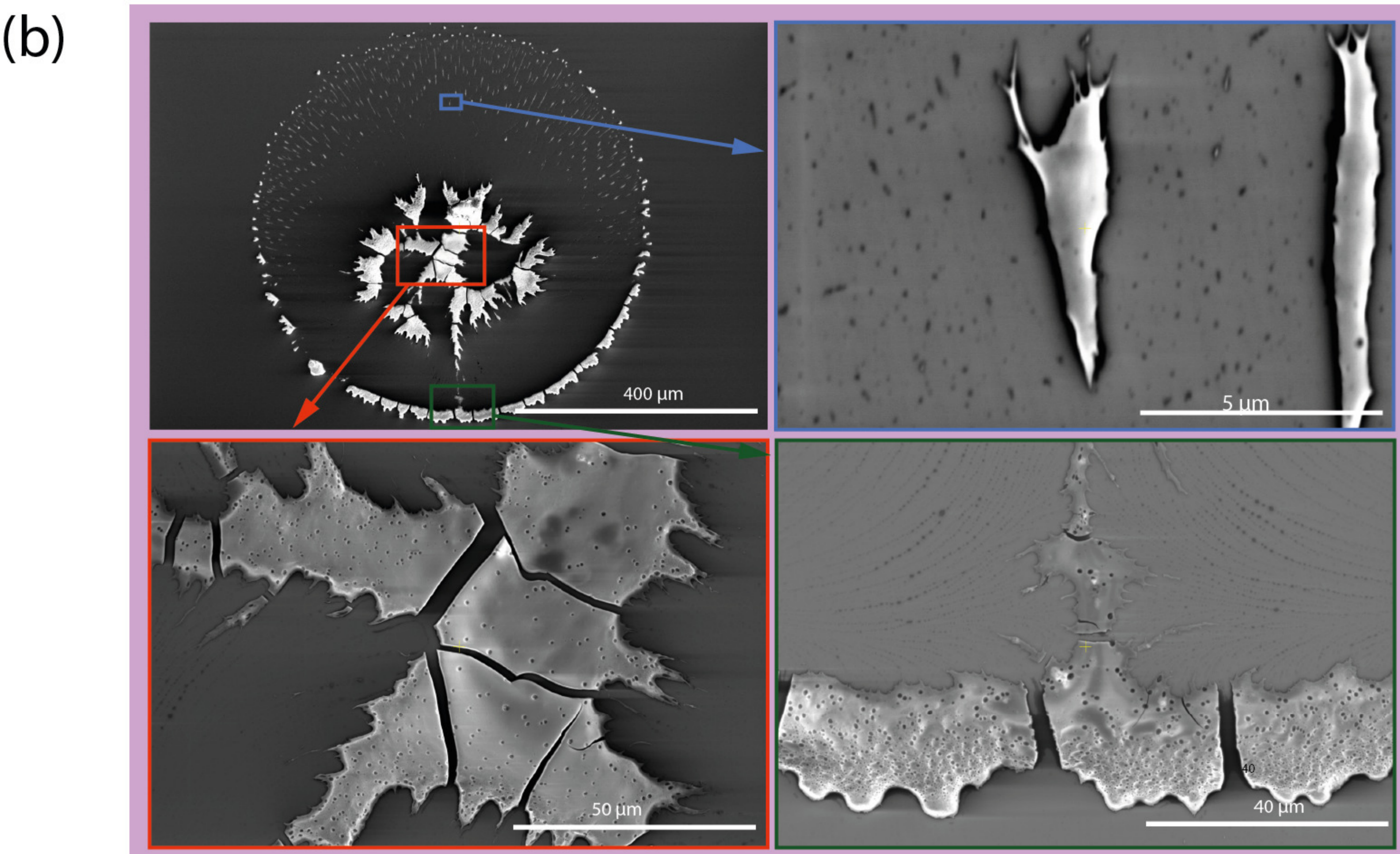
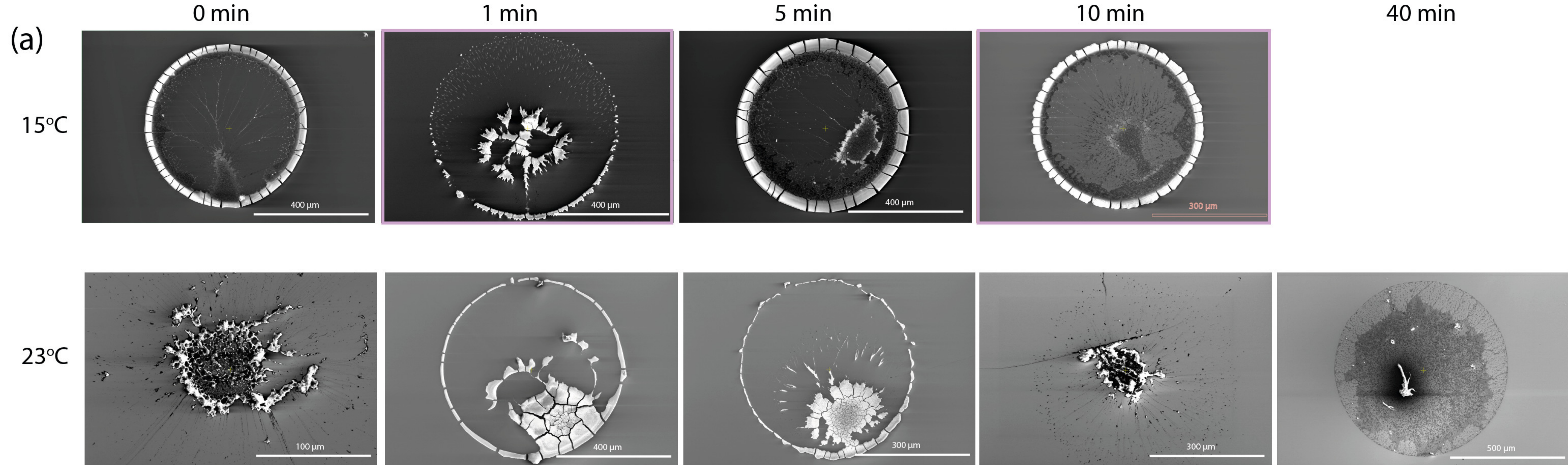


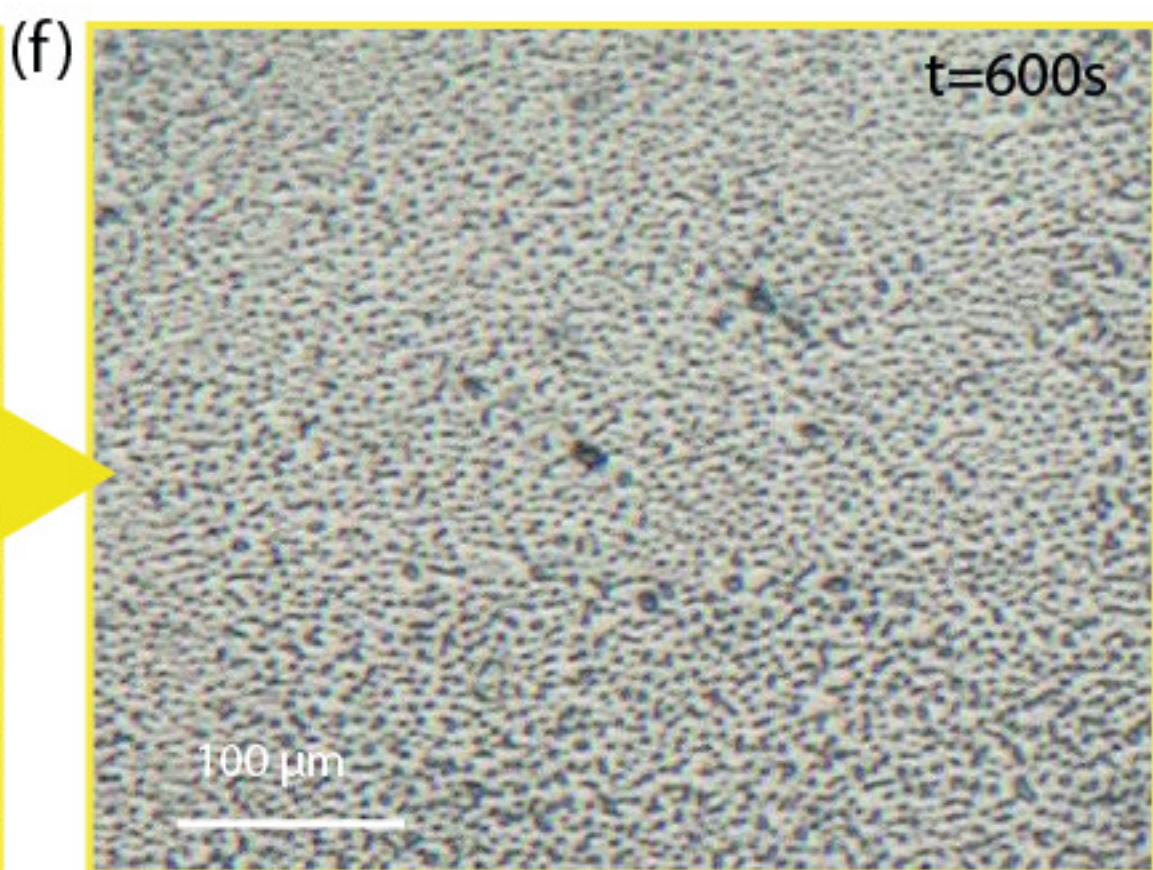
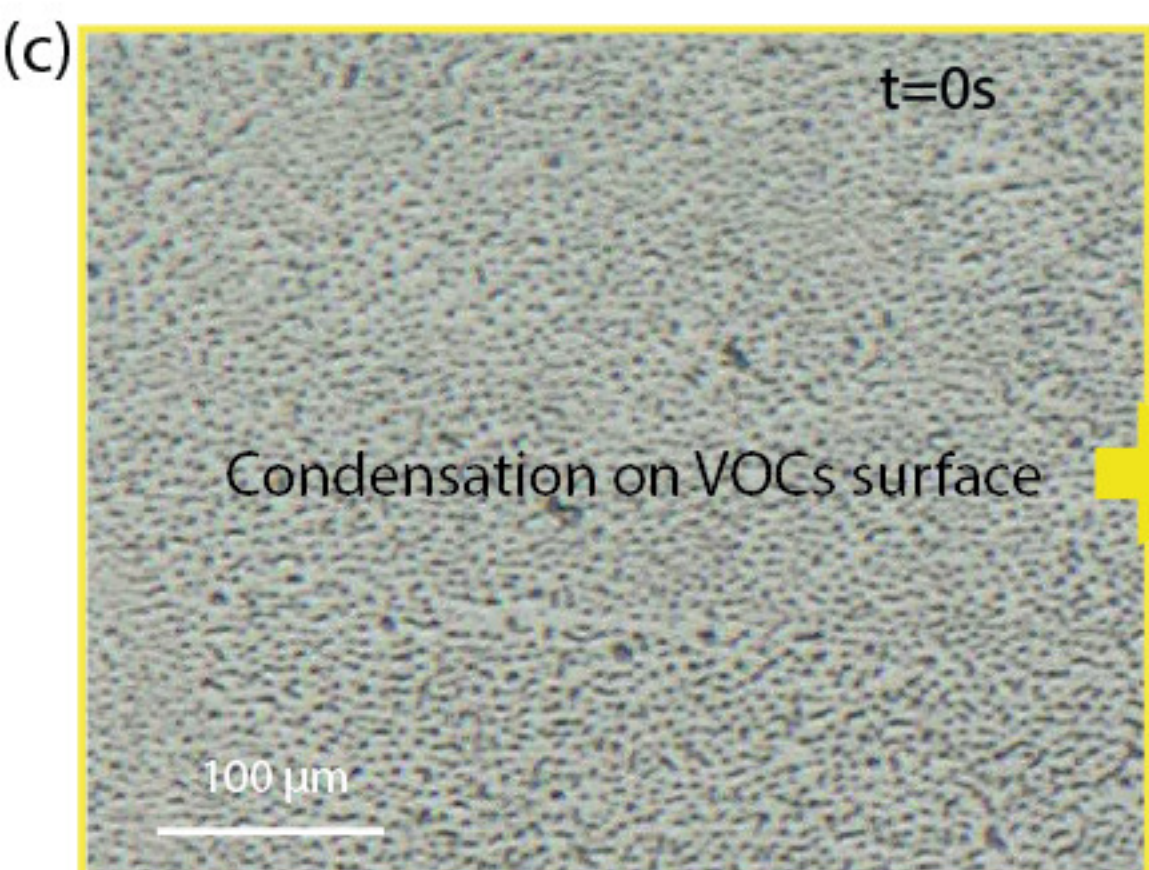
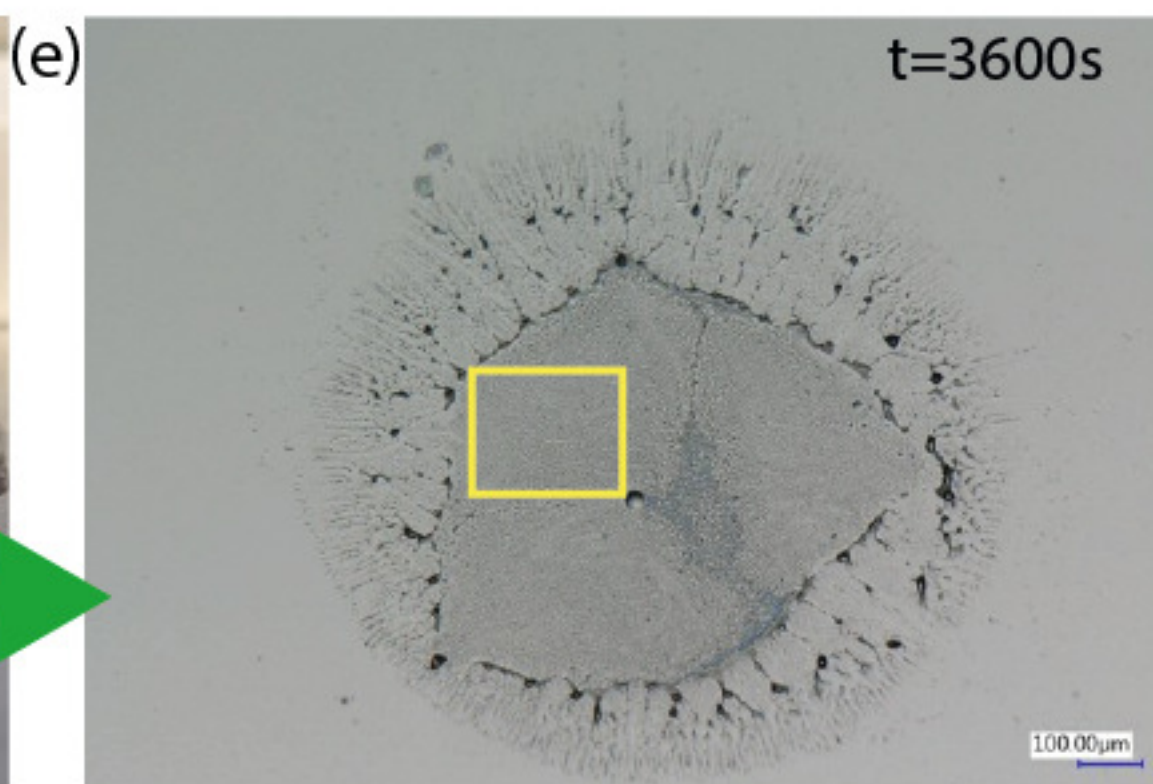
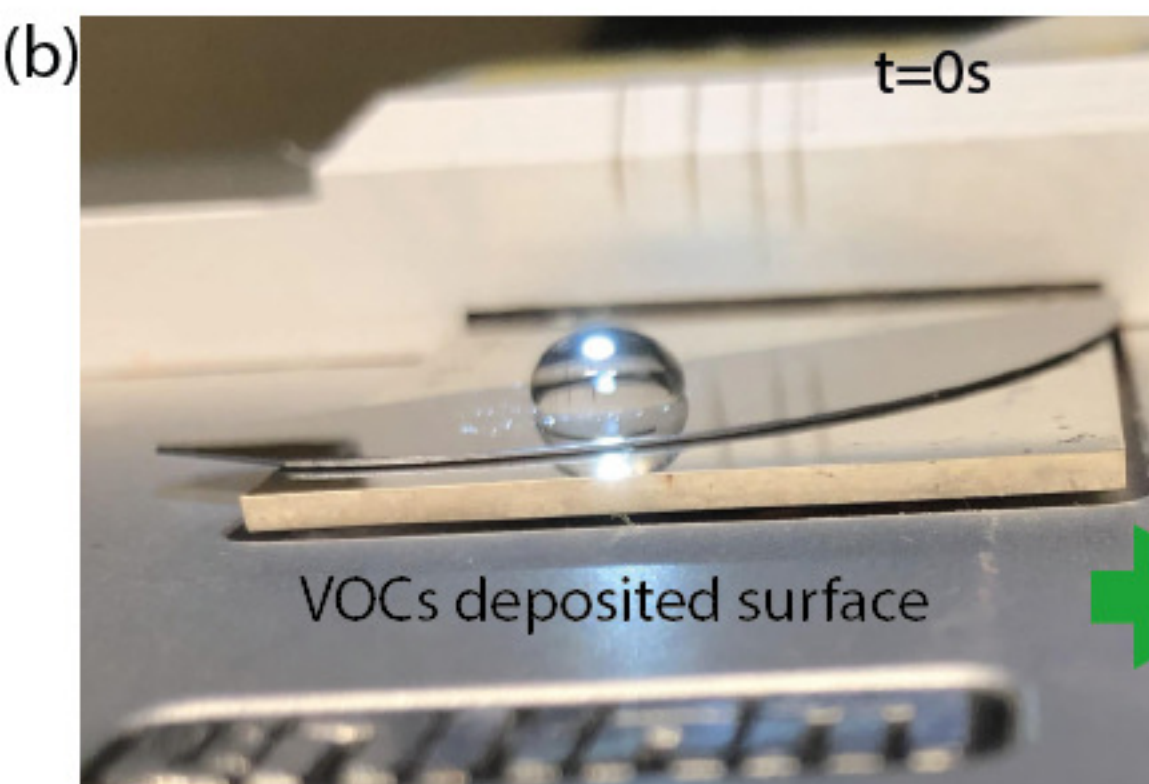
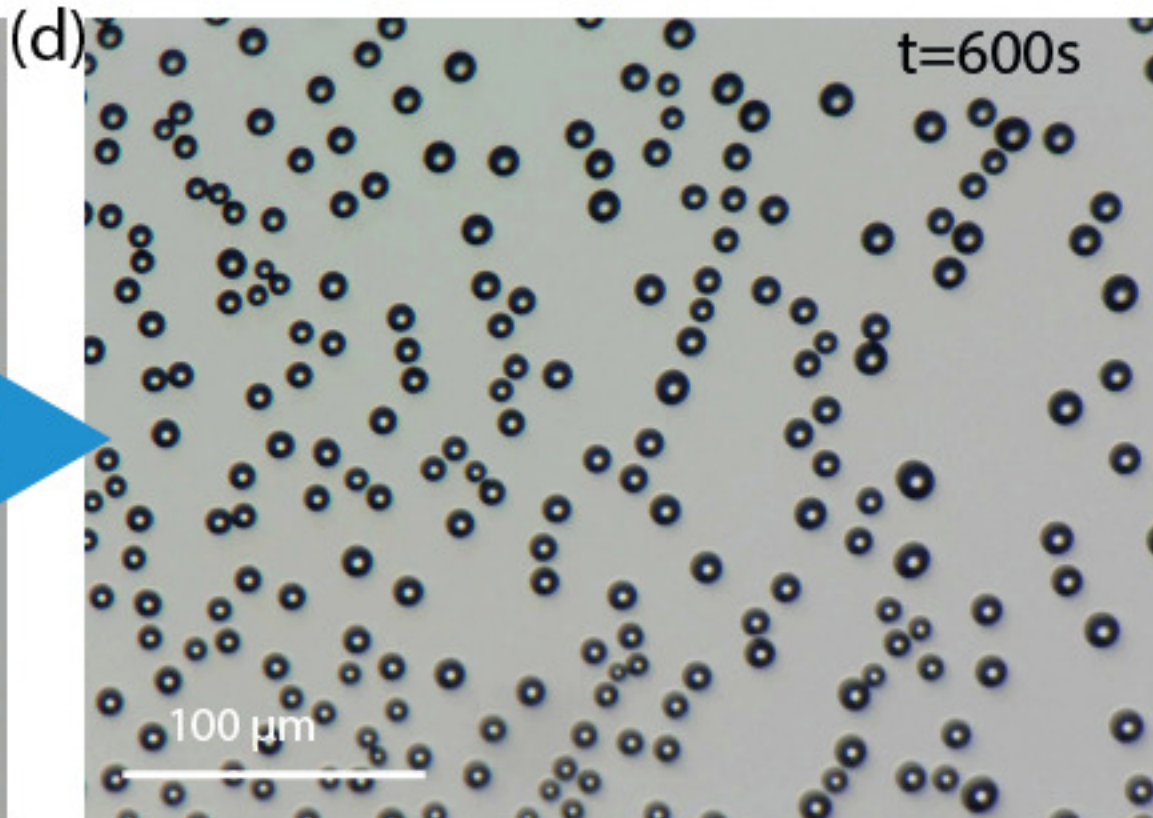
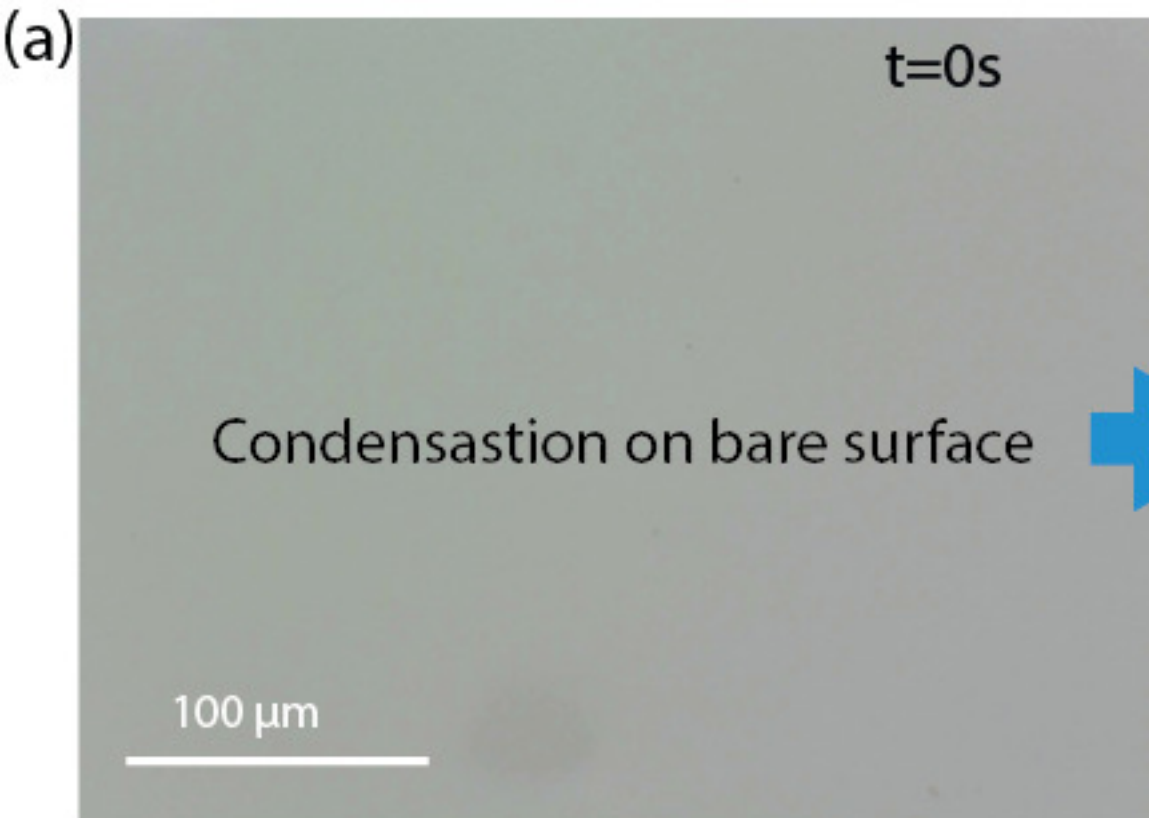
(c)



(d)







This is the author's peer reviewed, accepted manuscript. However, the online version of record will be different from this version once it has been copyedited and typeset.
 PLEASE CITE THIS ARTICLE AS DOI:10.1063/1.50056005

